Journal of Catalysis 263 (2009) 247–257

Contents lists available at ScienceDirect

Journal of Catalysis

www.elsevier.com/locate/jcat

Oniumsilica-immobilized-Keggin acids: Acidity and catalytic activity for ethyl *tert*-butyl ether synthesis and acetic acid esterification with ethanol

T.V. Kovalchuk [a], Ju.N. Kochkin [b], H. Sfihi [c,d], V.N. Zaitsev [a], J. Fraissard [c,e,*]

[a] *National T. Shevchenko University, Vladimirskaya 64, Kiev, Ukraine*
[b] *Institute of Physical Chemistry of NANU imeni Pisargevskogo, Kiev, Ukraine*
[c] *Laboratoire de Physique Quantique, ESPCI, 10 rue Vauquelin, 75005 Paris, France*
[d] *Département de Physique, UFR SMBH, University Paris 13, 74 rue Marcel Cachin, 93012 Bobigny Cedex, France*
[e] *University Pierre and Marie Curie, 4 place Jussieu, 75005 Paris, France*

ARTICLE INFO

Article history:
Received 29 April 2008
Revised 31 January 2009
Accepted 14 February 2009
Available online 14 March 2009

Keywords:
Keggin heteropolyacids
Acid onium salts
Surface-grafted cations
Oniumsilica-based HPA catalysts
Ethyl *tert*-butyl ether synthesis
Acetic acid esterification

ABSTRACT

Keggin heteropolyacids were immobilized on functionalized silica as their onium (γ-propyl-*N*-pyridinium, γ-propyl-*N*-methyl and γ-propyl-*N*-butyl-imidazolium) salts. Interaction between HPA and the surface-grafted onium cations affords acid salts. In contrast to bare silica, impregnated with HPA, these materials have monoanionic dispersions of HPA on the surface and superior resistance to HPA leaching in polar media. The greatest stability of the Keggin structure and resistance to leaching were found for $H_4SiW_{12}O_{40}$–(SiW)-, and the lowest for $H_3PMo_{12}O_{40}$–(PMo)-based samples. In the two model reactions tested, the liquid-phase synthesis of ETBE and the esterification of AcOH with EtOH, these solids display good catalytic performance (activity per anion, up to 150 and 25 h^{-1}, respectively) and relative high structural stability. Catalysts having a greater coverage of organic functions (revealed by comparing two pyridinium salts) and hydrophobic cations (by comparing two imidazolium salts) have the best performance. Amongst the heteropolyacids studied, $H_4SiW_{12}O_{40}$ is the most active and promising for catalyst design.

1. Introduction

With the aim of preparing new heterogeneous acidic catalysts based on HPA, we immobilized several HPA on onium cations grafted onto silica (SiO_2–Q). The preparation details, chemical characterization, anion distribution and porosity characteristics, as well as thermal stabilities of the solids prepared, are reported elsewhere [1]. The use of oniumsilica for preparation of catalysts resulted in a monoanionic dispersion of HPA on the surface, in contrast to the HPA, supported on pure silica. Ion exchange afforded acid salts with formulas $(SiO_2–Q)_{4-X}\cdot H_XA$ (SiW, SiMo) and $(SiO_2–Q)_{3-X}\cdot H_XA$ (PW, PMo). Use of tetraprotic acids, $H_4SiW_{12}O_{40}$ and $H_4SiMo_{12}O_{40}$, resulted in better surface exchange yields, greater acid site number per anion and strength. These solids are thermally stable up to 250–300 °C, with the highest thermal stability found for $H_4SiW_{12}O_4$ and $H_3PW_{12}O_{40}$. The present paper reports the acid properties of these materials (acid site number and strength), catalyst activity and stability under catalysis conditions. Activity was tested in two reactions demanding moderate acidity: alkylation of ethanol with isobutene (synthesis of ETBE) and esterification of acetic acid with ethanol (synthesis of ethyl acetate).

Methyl *tert*-butyl ether (MTBE) is a good octane number enhancer, and an ingredient for reducing CO and VOC emissions [2]. Ethyl *tert*-butyl ether (ETBE) is more attractive, because it can be produced from low-cost ethanol [2]. MTBE is produced commercially from MeOH and isobutene by a liquid-phase reaction using ion-exchange resins, such as Amberlyst, though Amberlyst suffers from low stability above 100 °C [3–5]. The key intermediate in ETBE (MTBE) syntheses from the corresponding alcohols and isobutene is the *tert*-butyl cation **1** that is formed by protonation of the latter according to Markovnikov's rule (Scheme 1). This reactive species interacts with EtOH (MeOH) to produce ethyl(methyl) *tert*-butyl ether **2**. Another oxygen nucleophile, i.e. water, which is normally present in the reaction mixture, may react with cation **1** in a similar way giving rise to *tert*-butanol **3** as a by-product. Ethanol itself under acidic conditions readily loses water to yield diethyl ether (DEE).

Many materials, such as zeolites and HPAs, have been studied as potential catalysts for MTBE (ETBE) synthesis [6]. HPAs proved to be active for MTBE and ETBE synthesis from isobutene and alcohols, as well as from *tert*-butanol [7]. The reaction can be carried out in homogeneous solution [8] or in the gas phase [9], using bulk [10] or heterogenized HPAs, such as carbon-supported

* Corresponding author at: University Pierre and Marie Curie, 4 place Jussieu, 75005 Paris, France.
E-mail address: jacques.fraissard@upmc.fr (J. Fraissard).

0021-9517/$ – see front matter © 2009 Published by Elsevier Inc.
doi:10.1016/j.jcat.2009.02.016

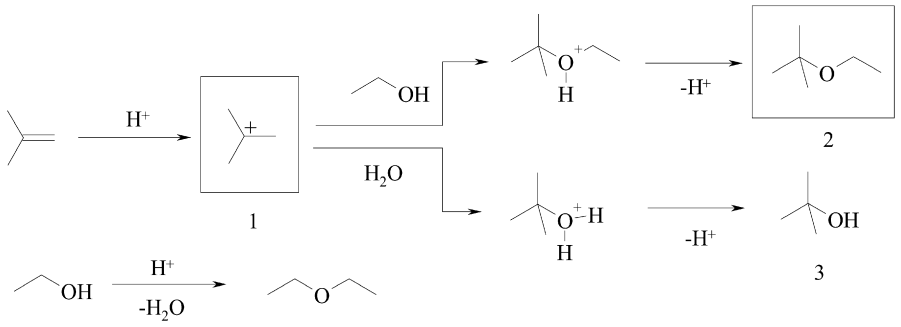

Scheme 1. Synthesis of ETBE from EtOH and isobutylene.

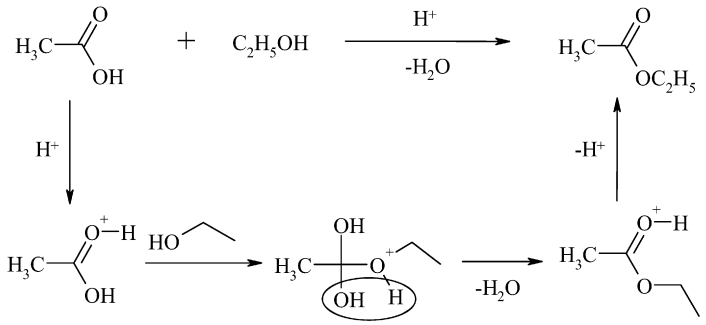

Scheme 2. Esterification of acetic acid with EtOH.

$Ag_3PW_{12}O_{40}$ [11], silica-supported HPAs [12] and polyaniline-immobilized $H_4SiW_{12}O_{40}$ [13]. The catalytic activity of several HPAs was shown to follow the order: $H_6P_2W_{18}O_{62} \gg H_4SiW_{12}O_{40} \approx H_4GeW_{12}O_{40} \approx H_3PW_{12}O_{40} > H_5BW_{12}O_{40} \approx H_6CoW_{12}O_{40}$ [9]. Amongst HPAs, Dawson acids display higher activity than Keggin acids [8]. For example, in gas-phase MTBE synthesis Dawson acid is active at 100 °C; its optimum pre-treatment temperature is around 150–200 °C, when the anion bears two water molecules [10].

The mechanisms and kinetics of the liquid-phase synthesis of MTBE from *tert*-butanol and MeOH [14], and of gas-phase ETBE formation from EtOH and isobutene [15] have been studied extensively. In the presence of a large excess of ethanol the reaction proceeds via the formation of the $C_2H_5^+$ cation and is first-order with respect to isobutene. The kinetic equation becomes more complex when the ethanol concentration is low: the reaction proceeds via the formation of the $C_4H_9^+$ cation. The presence of water in alcohols, in amounts equal to azeotropic, does not affect the equilibrium constants of ETBE and MTBE synthesis and can even increase the isobutene conversion [2]. Water, however, may inhibit the reaction until it is consumed to yield *tert*-butanol. It is noteworthy that the pseudo-liquid-phase behavior of HPAs and silica-supported HPAs plays a key role in MTBE synthesis, owing to the solvation of protons by methanol and suppression of the di(poly)merization of isobutene [16].

The esterification of carboxylic acids by alcohols is catalyzed by strong acids. Their role is to protonate the carbonyl group, which makes it far more electrophilic and reactive towards the alcohol (Scheme 2). As a result, the esterification of carboxylic acids became a convenient model reaction for evaluating the activity of solid acids.

Supported HPAs prove to be active catalysts for esterification. However, avoiding the leaching of HPA remains a challenge, so non-polar solvents, such as toluene, are often used. HPA immobilization on carbon involves strong interactions and provides leach-resistant and efficient catalysts in, for example, the esterification of propanoic acid with butanol and 2-ethylhexanol in toluene at 60 °C, with activities per anion of 3.6 and 6 h^{-1} for $H_4SiW_{12}O_{40}$ and $H_3PW_{12}O_{40}$, respectively [17]. Correlation of activity and HPA loading on several carbons shows that the activity per anion of carbon-immobilized HPA increases with the HPA loading and, for a given support, the best catalyst is the solid having the highest possible loading (as allowed by the interaction with the support) [18]. The activity is lower, however, than that of $H_3PW_{12}O_{40}$ in homogeneous media (activity per anion, 100–150 h^{-1}) and some HPA is leached from the catalysts.

Another way to prepare esterification catalysts starting with HPAs is to use siliceous supports, such as MCM-41. $H_4SiW_{12}O_{40}$ and $H_3PW_{12}O_{40}$ supported on MCM-41 are active in the liquid-phase esterification of benzoic acid with propan-1-ol in toluene, and the gas-phase esterification of acetic acid with butan-1-ol at 110 °C [19]. In the liquid phase esterification of benzoic acid with propan-1-ol, the activities per anion, calculated from the data given, are rather high: around 200–250 h^{-1} ($H_4SiW_{12}O_{40}$ is more active than $H_3PW_{12}O_{40}$). In as-prepared catalysts, HPA is well dispersed (no crystalline phase in XRD at 33 wt% of HPA), but the recycled catalysts show XRD reflections of bulk acid. Moreover, HPA crystals at least 10 nm in size (detected by TEM) are formed on the external pore surface, due to dissolution and recrystallization of HPA at the pore openings. These catalysts are active in the gas-phase esterification of acetic acid with butan-1-ol, with an activity per anion around 40 h^{-1} and selectivities of 85 and 80%, respectively (by-products are butane and Bu_2O). Clustering of HPA and darkening of the catalysts occur, as well as leaching of HPA from the solid, though it is less severe than in the liquid-phase esterification [20].

To the best of our knowledge, Keggin HPA-derived materials based on organosilicas functionalized with onium salts have not yet been reported as acid catalysts. The present study concerns the acidity and catalytic activity of four catalyst sets (**Py-1-HPA** and **Py-2-HPA**, **MeIm-HPA** and **BuIm-HPA**), prepared by ion exchange of siliceous supports (two different types of γ-pyridiniopropylsilica: **Py-1** and **Py-2**, γ-(*N*,*N*′-methylimidazolio)propylsilica **MeIm**, γ-(*N*,*N*′-butylimidazolio)propylsilica, **BuIm**) with four acids $H_3PMo_{12}O_{40}$ (denoted **PMo**), $H_3PW_{12}O_{40}$ (denoted **PW**), $H_4SiMo_{12}O_{40}$ (denoted **SiMo**) and $H_4SiW_{12}O_{40}$ (denoted **SiW**).

2. Experimental

2.1. Preparation

Silica (297.3 $cm^3\,g^{-1}$, 72 Å average pore size) was functionalized to have organic functions with the loadings as follows **Py-1:** 253 $\mu mol\,g^{-1}$ (pyridinium cation), 112 $\mu mol\,g^{-1}$ (chloropropyl groups); **Py-2**: 480 $\mu mol\,g^{-1}$ (pyridinium cation), 450 $\mu mol\,g^{-1}$ (chloropropyl groups); **MeIm**: 182 $\mu mol\,g^{-1}$ (methylimidazolium cation), 236 $\mu mol\,g^{-1}$ (chloropropyl groups); **BuIm**: 156 $\mu mol\,g^{-1}$ (butylimidazolium cation), 345 $\mu mol\,g^{-1}$ (chloropropyl groups). Onium silicas and HPAs were activated in vacuum at 150 °C for 4 h and at 80 °C for 2 h, respectively. A mixture of oniumsilica (2 g) and 10 ml of a ca. 0.1 M solution of HPAs (in MeCN for **Py-1** and **Py-2** and EtOH for **MeIm** and **BuIm**) was refluxed for 4–6 h, the solid separated by decantation, washed with the corresponding solvent, and the exchange procedure repeated twice. The samples were washed in a Soxhlet apparatus with MeCN or EtOH and dried under vacuum at 80 °C for 4–6 h. The onium salts of polyoxometalates prepared in this way are water-insoluble. After the extraction step and removal of physically adsorbed acid, no leaching of HPA occurs in either of the organic solvents or water.

Nitrogen adsorption [1] indicates that grafted onium-HPA salts almost retain the high specific surface areas of the starting silica. Pore diameter and volume decrease slightly, as compared to the starting silica. XRD does not show the presence of crystalline HPA in any sample prepared. The non-functionalized starting silica loaded with similar amounts of HPA via impregnation displays significant crystallinity. Measurements suggest a monoanionic distribution of HPA on the surface, expected to result from its chemical bonding to grafted silica.

2.2. Acid characterization

Acid site numbers were calculated from ammonia adsorption isotherms on samples activated at 200 °C for 5 h in nitrogen flow. Adsorption was performed at 25 °C (isotherm 1), followed by desorption in vacuum at 25 °C for 3 h (to a residual pressure of ±0.02 Pa over the sample for 0.5 h), and a second adsorption experiment (isotherm 2). The amount chemisorbed was calculated as the difference between the two isotherms, in $mol\,g^{-1}$ of the catalyst/starting silica. The acid site number was expressed as the number of ammonia molecules per Keggin unit of supported acid.

Acid site strength was evaluated from the chemical shift of adsorbed TEPO (triethylphosphine oxide) [21]. A sample (0.2 g) was added to a hexane solution of TEPO and kept at 60 °C for 5 h. Its ^{31}P SPE-MAS NMR spectrum was recorded after removal of the solvent by evaporation. Samples prepared in this way had TEPO concentrations of ca. 0.4 $mmol\,g^{-1}$ (**Py-1-HPA**, **Py-2-HPA**) and 0.2 $mmol\,g^{-1}$ (**MeIm-HPA**, **BuIm-HPA**).

The HPA concentration was determined by elemental analysis for both as-prepared and spent catalysts, including analysis of grafted organic groups. Elemental analyses were performed by the analytical laboratory of the CNRS, Lyon. The Mo and W contents were determined by X-ray fluorescence spectroscopy for samples diluted with H_3BO_3, by comparison of the data with a calibration set prepared with known concentrations of HPA and silica.

2.3. Catalysis

Synthesis of ETBE. The catalytic activity of **Py-1-HPA** and **Py-2-HPA** was tested in ETBE formation from isobutene and ethanol. The reaction was carried out under continuous flow, fixed-bed operating conditions at 10 atm and 60–160 °C. The catalyst was activated *in situ* at 120 °C in He flow at 1 Pa. Isobutene (10% in helium flow) and ethanol were first mixed in an ethanol:isobutene ratio of 1.5:1, and passed through the reactor cell filled with 1.5 cm^3 of catalyst (ca. 0.9–1.3 g). After stabilization at the reaction temperature (1 h), the products were collected for 15 min and analyzed. A commercial sample of Amberlyst-15 (sulfonic acid concentration, 4900 $\mu mol\,g^{-1}$) was used for calibration of the catalysis system. The reaction mixture was analyzed using a GC "Agate" Chromatron N-AW.

Esterification of acetic acid with ethanol was performed using **MeIm-HPA** and **BuIm-HPA**. The catalyst (0.2 g) was activated at 150 °C for 1 h and placed in a tightly closed Schlenk vessel charged with a mixture of AcOH (0.48 g, 8 mmol) and EtOH (1.47 g, 32 mmol). The substrate/catalyst ratio was ~400–800 (depending on the amount of HPA in the catalyst sample). The reaction mixture was vigorously stirred for 20 h at 60 °C. Conversion of acetic acid was measured by gas chromatography (IGC 12M chromatograph).

2.4. Spectroscopies

2.4.1. Infrared spectroscopy

DRIFT spectra with *in situ* thermal treatment were recorded on a Bruker Vector 22 spectrometer equipped with a Harrick diffuse reflectance cell, DTGS detector (400 scans, resolution 4 cm^{-1}, KBr background). Samples were diluted 1:10 with KBr, ground into fine powders and put in the reaction chamber without pressing.

2.4.2. NMR spectroscopy

^{31}P Single pulse excitation (SPE) and magic angle spinning (MAS) NMR measurements were performed at 202.47 MHz with a Bruker ASX 500 NMR spectrometer operating in a static field of 11.7 Teslas. The air-dried sample (as-prepared or spent reactivated samples were activated under vacuum at 80 °C for 4 h) was filled into a 4 mm zirconia rotor and spun at 5 kHz. The recycle delay was 30 s, in accordance with the phosphorus spin lattice relaxation times, and 64 scans were accumulated. The chemical shift was referenced with respect to external 85% H_3PO_4.

2.4.3. UV–vis spectroscopy

UV–vis adsorption spectra of HPA in solutions were acquired using a SPECOL 11 spectrophotometer from Carl Zeiss Jena. UV–vis diffuse reflectance spectra of solid samples were measured on a SPECORD M-40 at 12000–30000 cm^{-1}, using MgO background.

3. Results and discussion

3.1. Characterization of the chemical structure of fresh and spent catalysts

DRIFT measurements were used to follow the HPA structure in the catalysts after immobilization of HPA and in spent samples after catalysis tests. According to Fig. 1 (DRIFT spectra of a catalysts set **Py-2-HPA** with PW, SiW and PMo are shown as an example), in as-prepared catalysts HPAs keep the Keggin structure. Also, for the spent samples recovered after catalysis tests, the IR absorptions, in particular those due to HPA ($[PW_{12}O_{40}]^{3-}$: 980, 900, 815 cm^{-1}; $[SiW_{12}O_{40}]^{3-}$: 970, 924, 885, 805 cm^{-1}; $[PMo_{12}O_{40}]^{3-}$: 958, 885, 810 cm^{-1}), are unchanged. Moreover, the intensities of the respective absorptions are not decreased. According to IR data organic functions on oniumsilica are also stable under the catalysis conditions.

^{31}P SPE-MAS NMR spectroscopy provided more detailed information on the anion structure before and after tests. Spectra of some "as-prepared" and spent samples, containing the $[PW_{12}O_{40}]$ and $[PMo_{12}O_{40}]$ anions are shown in Figs. 2 and 3. As a rule, in the case of $[PW_{12}O_{40}]$-based catalysts only the peak at ca. −15 ppm,

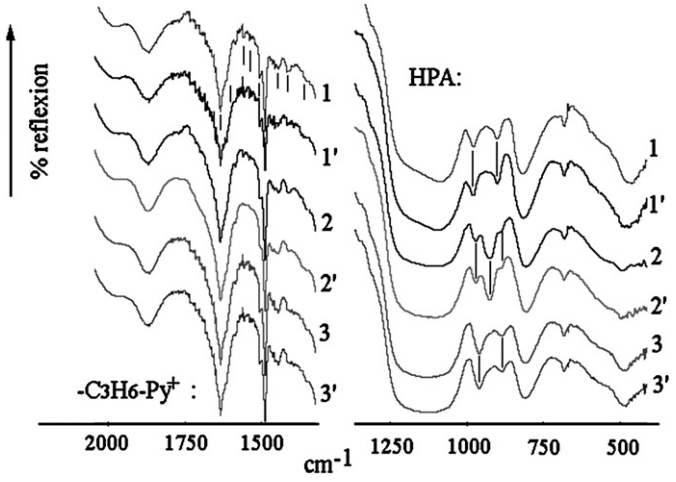

Fig. 1. DRIFT spectra (ambient conditions) of the Py-2-HPA catalyst set: **Py-2-PW** (1); **Py-2-SiW** (2); **Py-2-PMo** (3); spent samples, respectively (1′, 2′, 3′).

characteristic of the corresponding Keggin structure, was detected. In the case of samples with immobilized $H_3PMo_{12}O_{40}$, in addition to the peak of the intact Keggin anion at ca. −3.2 to −3.5 ppm, the spectra show another relatively weak peak at ca. 0–2 ppm, which was assigned to phosphate groups resulting from some decomposition of $H_3PMo_{12}O_{40}$. There is no significant difference between the chemical shifts of starting solid acid and immobilized anions, which indicates that in fresh catalysts the immobilized anions mostly have the intact Keggin structure. As in the spectra recorded for silica-adsorbed HPA [1], the peaks of Keggin anions are very narrow and symmetric. This suggests that no strong distortion of HPA is induced upon its bonding to the surface via onium salts.

On the whole, HPA in the spent catalysts used in both reactions retain their Keggin structure (peaks at −15 ppm for $H_3PW_{12}O_{40}$ and at −3.2 to −3.5 ppm for $H_3PMo_{12}O_{40}$). However, spectra of spent samples also contain other weak peaks due to decomposed Keggin anions. For $H_3PW_{12}O_{40}$-based catalysts these are at 0 ppm (phosphate anion) and at ca. −12 ppm; for $H_3PMo_{12}O_{40}$-based catalysts additional peaks are observed from 0 to −2 ppm. The latter peaks are, most probably, due to lacunary anions, with compositions PW_{12-x} and PMo_{12-x}. As NMR spectra show, the amount of lacunary species is more significant for catalysts prepared from $H_3PMo_{12}O_{40}$ (the corresponding peaks represent ca. 10% of the total intensity) than for $H_3PW_{12}O_{40}$-based catalysts (up to ca. 5% of the total intensity). Moreover, elemental analyses (C, H, N, P, Mo) performed on the spent catalysts (**Py-1-PMo** and **BuIm-PMo**, **MeIm-PMo**) show that the P:Mo ratio is close to 1:9–1:11 instead of 1:12.

The UV–vis spectra of fresh samples do not display any noticeable features around 600–800 nm that might be attributed to reduced heteropolyanions (so-called heteropolyblues; Fig. 4). The spent catalysts change in color from yellow to greenish (Mo-based samples) or from white to slightly yellow-brownish (W-based), evidencing partial reduction of heteropolyanions and/or their poisoning during their use as catalysts. This is accompanied in the spectra by the corresponding absorption bands near 550 nm (PW- and SiW-samples) and 710 nm (PMo- and SiMo-samples), while the main absorption bands are observed with the initial intensity. This reduction process is reversible, and the spent samples exposed to air regain their initial color in a few days.

3.2. Leaching stability

HPA concentrations in spent and as-prepared catalysts are presented in Tables 1 and 2. The concentrations are either unchanged (**Py-2-SiW**), fall slightly, by 5–9% (most PW-based and PMo-based catalysts), or considerably, by 21% (**Py-1-SiW**) and 35% (**BuIm-PMo**). Despite the strong chemical bonding of HPA to a grafted cation, its leaching could not be completely avoided. It must be noted, however, that the catalysts are tested under “rough” conditions, i.e. extremely polar media (AcOEt synthesis) and polar media in combination with high pressure and temperature (ETBE synthesis). It is important to note that HPAs supported on unfunctionalized silica cannot be used under these conditions, because all the HPA is lost during the first minutes of time-on-stream.

While the P/W ratio for most samples is close to 1:11, elemental analysis shows that the P/Mo ratio in Mo-based catalysts drops slightly to 1:9–1:11 (Table 2). Based on the ^{31}P SPE-MAS NMR results, we believe that most of the immobilized anions have the

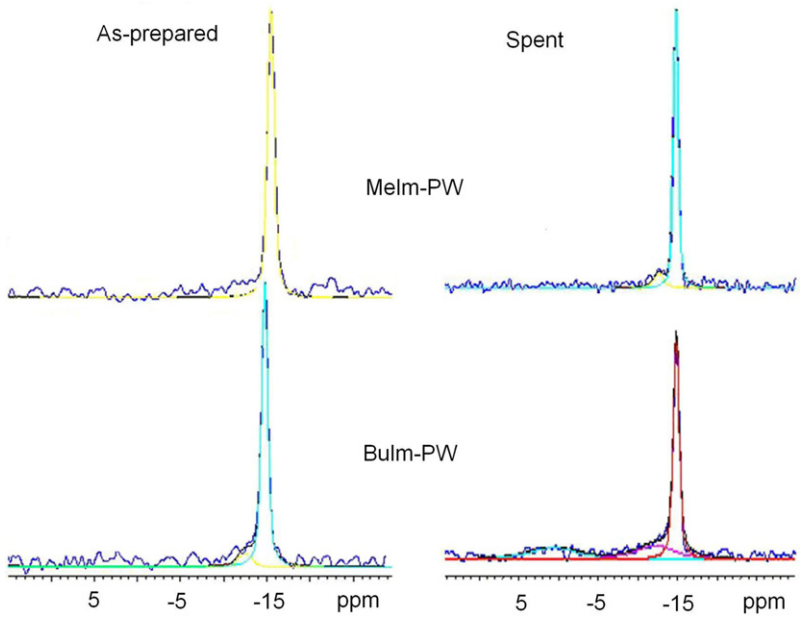

Fig. 2. ^{31}P SPE-MAS NMR spectra of $H_3PW_{12}O_{40}$ immobilized on **MeIm**, **BuIm** silicas: experimental spectra (noisy lines), individual fitted lines and their sum (non-noisy lines).

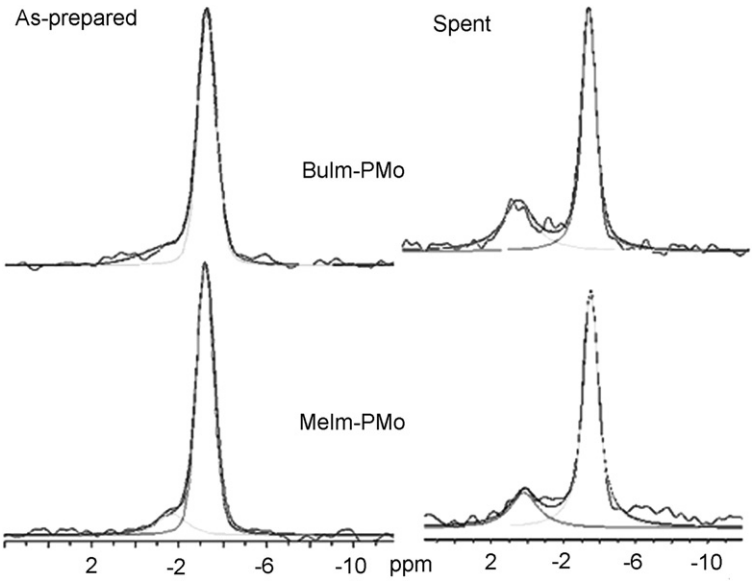

Fig. 3. ^{31}P SPE-MAS NMR spectra of $H_3PMo_{12}O_{40}$ immobilized on **MeIm**, **BuIm** silicas: experimental spectra (noisy lines), individual fitted lines and their sum (non-noisy lines).

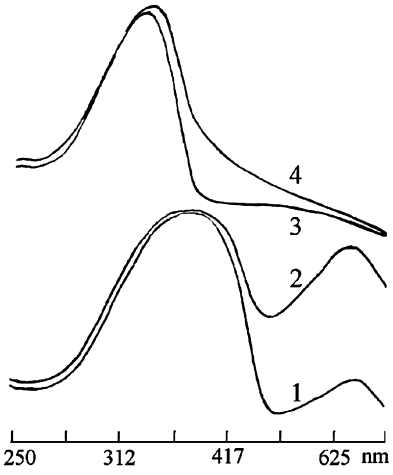

Fig. 4. UV–vis spectra of as-prepared catalysts: **Py-1-PMo** (1); **Py-1-SiW** (3) and of samples recovered after catalysis test, (2) and (4), respectively.

Keggin structure. At the same time, part of the PMo acid decomposes to primary oxides and undergoes transformation into lacunary anions, which effectively results in a decrease in the overall P/Mo ratio.

A slight increase in the carbon content (0.3–3%) was observed for all spent samples. This could be due to the irreversible adsorption of reactants or products, i.e. ethanol and isobutene or ETBE and DEE. Subsequently, due to an increase of sample weight after catalysis, the actual HPA loss is smaller than that calculated from elemental analysis.

In conclusion, the solids proved to be moderately stable when used as catalysts. We observed no decomposition of the grafted organic layer. Most of the immobilized heteropolyoxometalate retains the Keggin structure; however, some HPA (ca. 5–10%) is transformed into lacunary anions and phosphate ions. Moreover, a small fraction of the HPA is reversibly reduced (more pronounced in the case of molybdenum-based acid). The stability toward leaching depends on the HPA used: SiW- and PW-based solids are relatively stable (they lose HPA anions to a small extent), while the PMo-based solids are the least stable.

Table 1
X-ray fluorescence analysis on W-content: comparison of concentration of HPAs in as-prepared and spent catalysts (μmol g^{-1} of starting silica).

Catalyst	C (HPA), μmol g^{-1}, ±5		Loss (%)
	As-prepared	Spent	
Py-1-SiW	99	78	21.4
Py-1-PW	75	69	7.8
Py-2-SiW	151	150	0
Py-2-PW	102	93	8.7
MeIm-PW	47	44	5.9
BuIm-PW	70	66	5.3

3.3. Acidity measurements

The literature explains the acid properties of HPA salts by the following mechanisms:

(1) The acidity in the salts of group **A** can arise from an *acidic dissociation of coordinated water*, according to the equation:

$$M^{n+} + mH_2O \rightarrow \left[M(H_2O)_m\right]^{n+} \rightarrow \left[M(H_2O)_{m-1}(OH)\right]^{(n-1)+} + H^+.$$

For the salts of divalent cations the activity increases with the electronegativity of the cation, the activity of the trivalent salts going through a maximum on the curve of activity versus electronegativity [22]. For these salts, the activity is enhanced upon exposure to water. The formation of acid sites in this type of metal salt due to water dissociation was confirmed by pyridine adsorption [23].

(2) *Reduction of metal cations*. This mechanism occurs for the salts of the Pt family of metals, and proceeds according to the equation [23]:

$$Ag^+ + \frac{1}{2}H_2 \rightarrow Ag^\circ + H^+.$$

Water has no effect on acid site formation in this type of salt. Metal reduction and acid site generation can also proceed during the catalyzed reactions.

(3) *Inclusion of acid salts*. Conventional methods of preparation, such as the precipitation of salts, or drying of HPA solutions containing metal cations, can result in impure products, having some acid protons. If the surface area and the

Table 2
Elemental analysis for C, N, P, Mo concentration in catalysts (in wt% per g of catalyst). Concentrations of oniumpropyl (C_L) and HPA (C_L) are also given in μmol g^{-1} of starting silica (values in parentheses). The elemental analysis was done by the specialized French laboratory of the CNRS, Lyon.

Sample	C (%)	N (%) (C_L imidazolium)	P (%) (C_L phosphate)	Mo (%) (C_L)	Formula P/Mo
		MeIm-PMo			
As-prepared	2.15	0.46 (182 **MeIm**)	0.18 (64.2)	5.42 (624)	9.7
Spent	3.49	0.42 (165 **MeIm**)	0.16 (56.7)	5.11 (584)	10.3
Loss (%)	–	9.3	11.1	6.4	–
		BuIm-PMo			
As-prepared	2.85	0.40 (156 **BuIm**)	0.15 (53.0)	4.92 (562)	10.6
Spent	5.73	0.33 (126 **BuIm**)	0.12 (41.2)	3.31 (367)	8.9
Loss (%)	–	19	22	34.7	–
		Py-2-PMo			
As-prepared	5.15	0.61 (510 **Py**)	0.26 (98)	8.6 (1044)	10.7
Spent	5.45	0.60 (499 **Py**)	0.28 (105)	8.0 (972)	9.2
Loss (%)	–	2	–	6.9	–

acidity of the precipitate are high enough, an active catalyst can be obtained. The most important of this type of catalyst is $Cs_{2.5}H_{0.5}PW_{12}O_{40}$, which precipitates upon addition of an aqueous solution of Cs_2CO_3 to $H_3PW_{12}O_{40}$ [16]. This was the first of a new class of microporous HPA-based catalysts, claimed to have superacidity together with high hydrophobicity [16,24–29].

(4) *Partial hydrolysis of anions* can occur during the preparation and/or immobilization. This changes the anion structure, resulting in the formation of acid protons:

$$H_3PW_{12}O_{40} + 3H_2O \rightarrow \left[PW_{11}O_{39}\right]^{7-} + WO_4^{2-} + 9H^+.$$

(5) *Lewis acidity of the counterion in HPA*. Apparently, of the five mechanisms describing the development of acidity in HPA salts, the acidity of surface-grafted HPA onium salts is expected to be determined either by mechanism (3), and depend on the proportions of onium cation, proton and HPA anion, or by mechanism (4): partial HPA hydrolysis.

3.3.1. Acid site number by NH_3 adsorption

According to the literature, pure HPAs irreversibly adsorb up to six molecules of pyridine or three molecules of NH_3 per Keggin unit (KU) at 25 °C [30]; three molecules of pyridines are retained by HPA after evacuation at 130 °C and this agrees with the number of protons [31]. The acid salts of alkali metals also irreversibly bind pyridine at 130 °C, but in smaller amounts (0.5–2 molecules per KU). Neutral salts, such as $Na_3PW_{12}O_{40}$, $Cu_{3/2}PW_{12}O_{40}$ and $Cs_3PW_{12}O_{40}$, irreversibly bind 1.2, 2 and 0.3 pyridines per KU, respectively [31].

In our case, the number of ammonia molecules adsorbed per KU of onium-HPA salts approaches six, see Table 3 (except for sample **Py-2-PMo**). The number of NH_3 molecules adsorbed at 25 °C is therefore extraordinarily high.

Both possible ways for acid site generation: acid salt inclusion, (3) and anion hydrolysis, (4), will result in the formation of Brønsted sites. Our results (NMR and EA) have indicated toward the hydrolysis of immobilized acid, but to some extent only, so this is barely the main reason for the increase in acid site number. Moreover, immobilization of HPA via their onium salts should decrease the initial number of protons by KU at least by one. Thus, the excess of ammonia adsorption under the experimental conditions must be due to another mechanism, different from the adsorption on Brønsted acid sites. In the absence of air/moisture under ammonia atmosphere, W/Mo(VI) coordinatively bind with ammonia. Such a donor–acceptor interaction can be considered in terms of Lewis acid/Lewis base interaction, where the Lewis acid is an electron pair acceptor W/Mo(VI) and the Lewis base an electron pair donor (:NH_3). This mechanism has been described by Damyanova

Table 3
Amount of adsorbed NH_3 on **Py-HPA** catalysts: (1) per gram of functionalized silica; (2) per gram of starting silica; (3) per mole of immobilized acid, which is assumed to be equal to the number of acid sites per Keggin unit (KU).

Catalyst	(1) C NH_3, μmol g^{-1} catalyst	(2) C NH_3, μmol g^{-1} SiO_2	(3) NH_3/KU
Py-2-PMo	900	1100	14.8
Py-2-PW	550	725	5.7
Py-2-SiW	500	735	5.8
Py-1-SiW	400	520	5.3
Py-1-PW	400	495	6.6

to explain the observation of Lewis acid sites during pyridine adsorption by silica-immobilized HPA [32].

The suggested interpretation is supported by the following observation. Adsorption of NH_3 is accompanied by an immediate change in the initial color of the HPA onium salt, white (W) or greenish-yellow (Mo) to pale yellow-brown. Upon exposure to air, the initial color of the sample is slowly regained. As a conclusion, there are two types of adsorbed ammonia: ammonia which irreversibly interacts with Brønsted sites and reversibly coordinated ammonia. Thus, our experiments indicate that, for the studied catalysts, HPA-onium salts, the number of adsorbed ammonias does not directly reflect the number of Brønsted acid sites.

The **Py-2-PMo** catalyst (14.8 NH_3 molecules adsorbed per KU) is a case apart. The generation of additional Brønsted sites for this sample can result from mechanism (4): hydrolysis of the Keggin anion (this sample was shown by ^{31}P SPE-MAS NMR to decompose to a greater extent). HPA in other samples have mainly Keggin structures, as confirmed by FTIR and ^{31}P SPE-MAS NMR, so this mechanism does not apply.

3.3.2. Acid site strength by ^{31}P SPE-MAS NMR of adsorbed TEPO

The ^{31}P chemical shift of TEPO adsorbed on solid acids depends on the acidity of the surface sites and, therefore, can be used for its determination [21]. A phosphorus of TEPO physisorbed on silica has a chemical shift in the 50–56 ppm range. This value was used as a reference for a non-acidic solid.

In this work, TEPO physisorbed on a support (**Py-1**) displays one sharp peak at 59 ± 0.5 ppm ($\Delta\nu$ $\frac{1}{2}$ 250 Hz, Figs. 5 and 6). The sharpness of the signal results either from the similar environment of TEPO adsorbed on silanol sites and thus a narrow chemical shift distribution, and/or from the mobility of TEPO in a hydroxyl network due to the hydrophilicity of the surface.

^{31}P SPE-MAS NMR spectra of TEPO adsorbed on the catalysts show a strong broad peak which is fitted with two mixed Gauss–Lorenz curves: (1) at ca. 60 ppm ($\Delta\nu$ $\frac{1}{2}$ 600–1200 Hz), and (2) at ca. 70–80 ppm ($\Delta\nu$ $\frac{1}{2}$ 1300 Hz). Some of the spectra exhibit an additional, weak peak at ca. 95–110 ppm. These three peaks re-

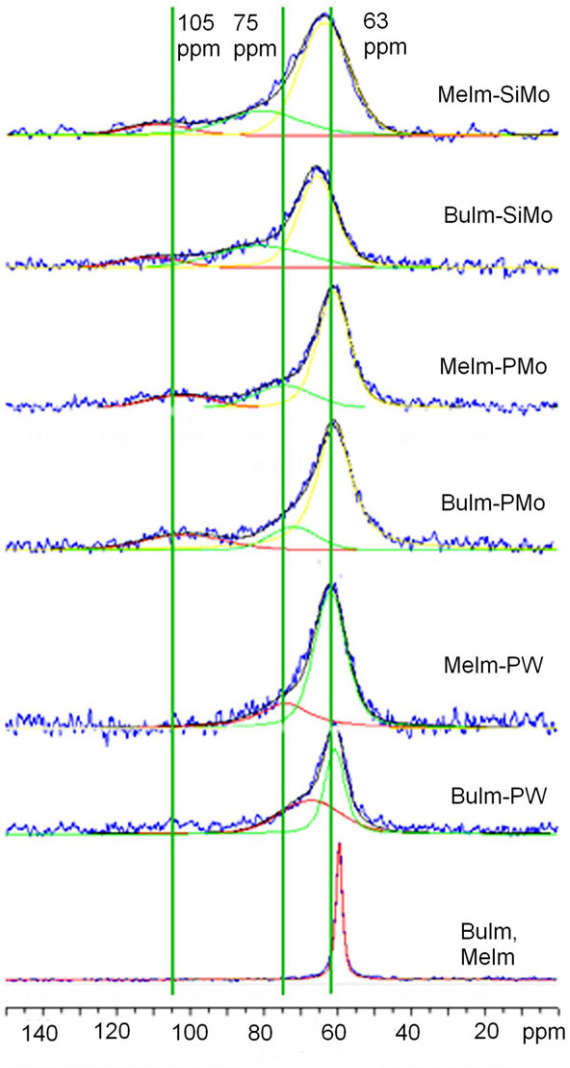

Fig. 5. ^{31}P MAS NMR spectra of TEPO adsorbed on HPA-imidazolium-silicas.

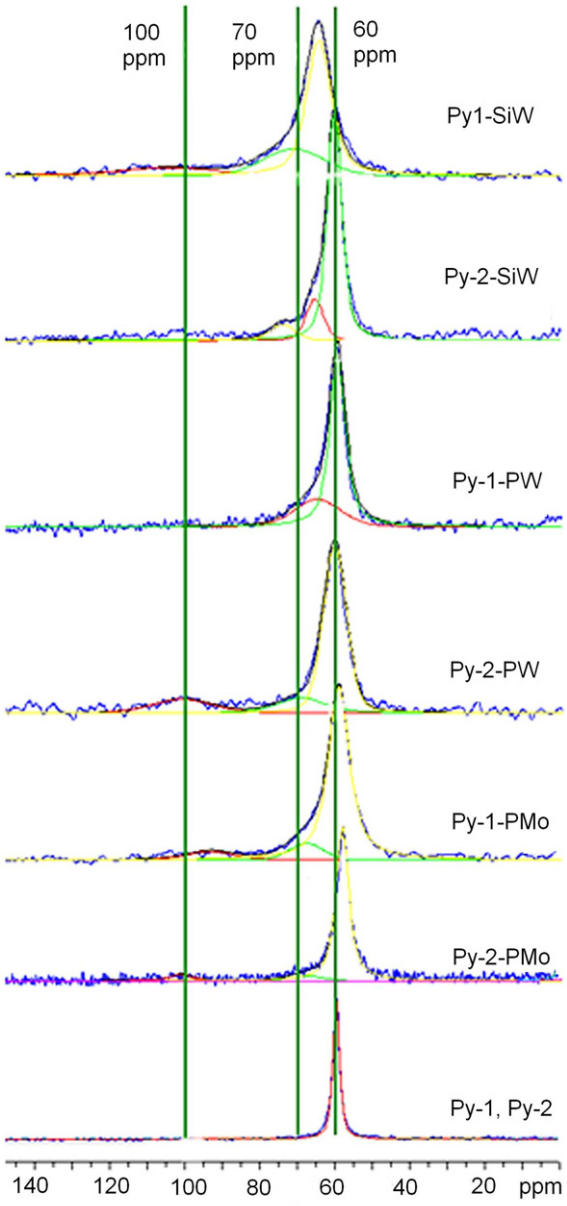

Fig. 6. ^{31}P MAS NMR spectra of TEPO adsorbed on HPA-pyridinium-silicas.

veal the existence of three different types of surface sites. As in the spectra of TEPO on the support, the peak at ca. 60 ppm is attributed to TEPO adsorbed on surface silanols. However, this peak is much broader and located 1–6 ppm upfield of TEPO adsorbed on the starting silica. This is probably due to an interaction between the HPA sites and silanols, resulting in a wider distribution of acidity of these sites. The two other peaks most probably correspond to TEPO adsorbed on acid sites of moderate (ca. 70–80 ppm) and higher acidity (ca. 95–110 ppm). For triprotic heteropolyphosphonic acids, the moderate-acidity sites can have the formula $(SiO_2–Q)_2{\cdot}HA$, whereas the stronger sites can be those with the formula $SiO_2–Q{\cdot}H_2A$. For tetraprotic heteropolysilicic acids, the moderate-acidity sites can have the formula $(SiO_2–Q)_3{\cdot}HA$, $(SiO_2–Q)_2{\cdot}H_2A$, whereas the stronger acid sites can be those with the formula $(SiO_2–Q){\cdot}H_3A$. The acidity of the bulk HPAs used as precursors is known to increase in the following order:

$$H_4SiMo_{12}O_{40} < H_3PMo_{12}O_{40} < H_4SiW_{12}O_{40} < H_3PW_{12}O_{40}.$$

According to the chemical shifts of the adsorbed TEPO, the acidity of the immobilized HPAs, decreases as follows:

Support	Acid	Support	Acid
Py-2:	PMo ≈ < PW < SiW	**Py-1**:	PMo < PW < SiW
MI-1:	PW ≈ < PMo ≪ SiMo	**BI-1**:	PW ≈ < PMo ≪ SiMo

The most upfield chemical shifts (greatest acid site strength) were observed for the immobilized tetraprotic acids $H_4SiW_{12}O_{40}$ and $H_4SiMo_{12}O_{40}$. These salts are likely to have more acid protons per one immobilized Keggin unit.

The ratio of the relative intensities of the ^{31}P SPE-MAS NMR peaks of TEPO adsorbed on acid centers (peak at 70–110 ppm) to those due to the Keggin anion allows us to estimate the number of TEPO molecules associated with one Keggin unit. This value is equal to the number of acidic protons per KU available for interaction with TEPO (ca. 0.3–1).

3.3.3. Thermal decomposition and secondary adsorption of pyridine on immobilized samples by IR

IR spectra of adsorbed pyridine have been widely used to characterize the acid sites in solid acids [31–34]. The spectra of pyridine adsorbed on Brønsted sites usually include bands at 1485–1500, 1540 and 1640 cm^{-1} (pyridinium cation) and hydrogen-bonded pyridine at 1400–1477, 1485–1477 and 1485–1490 cm^{-1}. The adsorption of pyridine on Lewis sites is characterized by the band around 1440–1445 cm^{-1}. The spectra of protonated pyridine

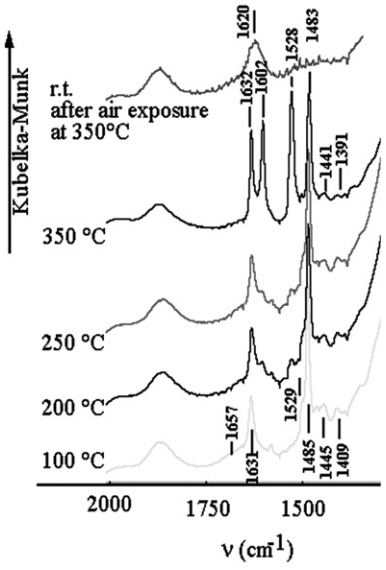

Fig. 7. DRIFT monitoring of the decomposition of Py-2-SiW in N_2 flow.

and ammonia in bulk $H_3PW_{12}O_{40}$ and its Cs salts, as well as those of the precipitated salt $(C_5H_5NH^+)_3PW_{12}O_{40}$, have been described and assigned [35]: its spectrum exhibits absorptions at 1640, 1605–1615 (split into two), 1530–1542 (split into two), 1487 cm^{-1}.

Initially, in the spectra of catalysts we observe bands at 1630–1635, 1480–1483 cm^{-1} (ring stretch in pyridinium ion) and 680–682 cm^{-1} (pyridine fingerprints), due to the pyridinium cation in the grafted salts $-C_3H_6C_5H_5N^+$–HPA (Fig. 7). During thermal treatment (200–350 °C) new strong bands appear at 1602, 1525–1528 cm^{-1} (ring stretch in pyridinium ion or H-bonded pyridine) as well as 752–758 cm^{-1} (pyridine fingerprints) [1]. The new absorptions appear as a result of the decomposition of grafted SiO_2–$C_3H_6C_5H_5N^+$–HPA, (and, probably, SiO_2–$C_3H_6C_5H_5N^+$–Cl^-) salts. Decomposition of grafted pyridinium cation results in formation of pyridine molecule. Pyridine, however, does not evolve from the sample due to interaction with HPA. The spectra of the thermally transformed samples are comparable to that of pyridine chemisorbed on bulk HPA and of the precipitated $(C_5H_5NH^+)_3PW_{12}O_{40}$ [35]. Protonated pyridine is held strongly on the surface (up to 300–350 °C in N_2 flow) and is desorbed during decomposition in air at 350 °C. There are also bands in spectra due to adsorbed pyridine in the C–H and N–H stretching region at 3204–3206, 3051 and 3140–3142 cm^{-1} but their assignment is difficult.

During thermal treatment a small band at 1445–1441 cm^{-1} is observed, which can be assigned to pyridine adsorbed on Lewis sites, but seems to be negligible in our study.

3.4. Catalytic activity

3.4.1. Synthesis of ETBE

The activities of catalysts based on pyridiniopropyl-silicas were evaluated in ETBE synthesis starting from EtOH and isobutene (Table 4). Firstly, a pilot catalyst was tested. The pH of the eluate obtained at the beginning of the reaction (at 100 °C) showed some leaching of acid, which, however, fell in the subsequent tests at higher temperatures. To minimize the risks of leaching under the reaction conditions, all catalysts were washed with hot MeCN/EtOH in a Soxhlet apparatus for 12 h prior to the tests.

Bulk silica and pyridinium-silica without bonded acid (blank reaction) were inactive in the conversion of isobutene. In contrast, all catalysts prepared displayed high activity, depending both on the nature of the immobilized HPA and of the support. All $H_3PMo_{12}O_{40}$-based catalysts have low activities (activity per anion, 2–30 h^{-1}). This is probably due to the precursor acid having the lowest acidity. As expected from the acidity measurements and the known order of activity of the precursor acids, the highest conversion and best selectivity to ETBE, is obtained for immobilized $H_4SiW_{12}O_{40}$: **Py-1-SiW** and **Py-2-SiW** (activity per anion, 10–150 h^{-1}). **Py-1-PW** and **Py-2-PW** catalysts are somewhat less active (activity per anion, 5–60 h^{-1}). In agreement with the results reported for pure and supported acids, $H_4SiW_{12}O_{40}$-onium catalysts are more active than the corresponding $H_3PW_{12}O_{40}$ catalysts [9,17,36]. The greater softness of the corresponding $[SiW_{12}O_{40}]^{4-}$ anion can be an important factor contributing to its activity. Moreover, in our case, the greater activity can also be related to the larger number of residual protons in the acid salts formed between tetraprotic acid and oniumsilica $[Py_{4-x}H_xSiW_{12}O_{40}]$, and the higher acid site strength of the corresponding catalysts, as measured by the ^{31}P SPE-MAS NMR of TEPO.

Regarding the two supports used, higher conversions and activity per anion are obtained for the pyridinium-silica **Py-2** with a polymerized (cross-linked) layer, having a greater degree of functionalization and HPA loading than **Py-1**, probably mostly due to better lipophilicity.

Conversion of isobutene to ETBE (1–67%), per weight unit of the solid, is lower for all the samples studied than for the commercial catalyst, Amberlyst-15 (39–78%, at temperatures suitable for the latter). However, when the catalyst activity is transformed into activity per anion unit (mole of isobutene per mole of KU per h, for Amberlyst-15 normalized to the concentration of sulfate groups), it is obvious that the activity of Py-1(2)-HPA solids (2–150 h^{-1}) exceeds that of the commercial catalyst (2–4 h^{-1}). Good accessibility of the acid sites on the functionalized silica surface, as suggested by the excellent dispersion (BET results), as well as the additional stabilization of the carbocation by HPA, may explain why the activities per anion for HPA-based catalysts are much higher than for the reference sample, a polymeric support containing a sulfonic acid. The maximum activity is reached at 120–160 °C. At this operating temperature (>120 °C) the application of Amberlyst-15 is limited because of its decomposition.

A relatively good selectivity to ETBE (70–85%) is attained with all catalysts, and is equal to or slightly better than that displayed by Amberlyst-15. The selectivity to ETBE increases with the temperature, whereas that to *t*-BuOH decreases. However, with the two most active and "acidic" samples, **Py-1-SiW** and **Py-2-SiW**, at high temperature (160 °C) the reaction becomes less selective, Et_2O being produced (selectivity 10–15%). None of these materials catalyzes isobutene oligomerization.

ETBE synthesis, an exothermic reaction, is reported to proceed easier in the low-temperature region and to be inhibited at high temperatures. In our experiments, the activities of the catalysts develop with increasing temperature, though in different ways. Up to 85 °C, the activities of $H_3PMo_{12}O_{40}$-based catalysts decrease and then increase steadily. The activities of $H_4SiW_{12}O_{40}$-based catalysts increase continuously, reach a maximum at 110–135 °C, and then decrease. This performance is possibly related to several factors: exothermicity of the reaction, increase in the acid strength with dehydration of the catalyst, and partial loss of HPA occurring under the reaction conditions used, at increasing temperatures and high pressure. As indicated in Tables 1–2, X-ray fluorescence and elemental analysis showed almost no loss (**Py-2-SiW**), slight loss, by 5–9% (PW-based and PMo-based catalysts), and a more considerable loss of 21% (**Py-1-SiW**) (Tables 1 and 2). Consequently, this variation is due to the two first factors without it being possible to separate their influence.

Comparison with known HPA-based catalysts. When pure oxides are used as $H_4SiW_{12}O_{40}$ supports to prepare solid catalysts for gas-phase synthesis of MTBE from isobutene and methanol, the activity

Table 4
Results of the catalysis tests in ETBE synthesis from isobutene and EtOH. Activity per anion (mol product per mol KU per h) in ETBE synthesis.

Support	Acid	T (°C)	Conversion of isobutene (%)	Selectivity, % ETBE–% *t*-BuOH–% DEE	Activity per anion (h^{-1})
Py-1	PMo	60	3.1	82–18–0	15
		85	0.8	100–0–0	1.5
		110	0.6	100–0–0	1
		135	3.3	78–22–0	8
		160	13.7	92–8–0	34
	PW	60	6.8	85–15–0	8
		85	0.7	100–0–0	2
		110	1.0	100–0–0	3
		135	5.8	78–22–0	14
		160	24.1	90–10–0	60
	SiW	60	6.7	72–28–0	10
		85	43.5	79–21–0	81
		110	66.6	80–20–0	150
		135	45.5	85–15–0	92
		160	32.9	70–15–15	73
Py-2	PMo	60	12.3	78–22–0	26
		85	2.6	72–28–0	5
		110	3.1	88–12–0	6
		135	7.5	80–20–0	12
		160	11.9	75–15–0	23
	PW	60	2.5	70–30–0	5
		85	5.4	77–23–0	10
		110	20.0	79–20–0	40
		135	26.0	85–15–0	48
		160	21.0	90–10	41
	SiW	60	4.2	80–20–0	7.5
		85	9.3	79–21–0	13
		110	40.0	82–18–0	64
		135	31.0	85–15–0	46
		160	23.0	80–10–10	35
Amberlyst		60	39.0	60–25–15	1.9
		80	59.0	80–20–0	2.9
		100	71.0	80–20–0	3.3
		120	78.0	78–22–0	2.8
		140	67.0	77–23–0	3.2

depends on the support basicity as well as the degree of surface coverage with HPA [37]. Strongly basic supports decrease the activity of HPA, in terms of activity per anion, so silica gives better catalysts than alumina. Such catalysts exhibit 5–40 h^{-1} activity per anion, depending on the support and temperature, the best results being obtained at low temperatures. As reported in [37], the activity per HPA unit on all supports diminishes when the degree of surface coverage exceeds 1.5 monolayers. The selectivity to ETBE is lower than 100% and *tert*-butanol is formed as a by-product.

Using strong electrostatic interaction with oniumsilicas, we have prepared catalysts which perform noticeably better (10–150 h^{-1}, for example, for $H_4SiW_{12}O_{40}$) than silica-supported acid (5–40 h^{-1}). The higher activity achieved per anion is probably due to the fact that the HPA, although it has lost in acidity, gains significantly in the dispersion and accessibility of the acid sites [1].

The catalysts reported here are related to that prepared by immobilization of $H_4SiW_{12}O_{40}$ on polyaniline for gas-phase MTBE synthesis from isobutene and methanol [13]. This catalyst was shown to have good accessibility of $H_4SiW_{12}O_{40}$, excellent performance and to give higher conversion than a bulk acid. However, $H_4SiW_{12}O_{40}$ adsorbed on polyaniline was reported to adsorb isobutene irreversibly (up to 17 monolayers on the surface). Eventually, oligomers are produced, causing catalyst darkening at temperatures higher than 90 °C. Moreover, this gave lower selectivity to MTBE (75–85%) than that obtained with pure HPA. Probably the monoanionic HPA dispersion impedes achievement of "the pseudo-liquid phase", as for pure HPAs, where protons are solvated by methanol, which suppresses the di(poly)merization of isobutene.

In our study, the selectivity to ETBE using oniumsilica-immobilized HPAs is comparable to that achieved with $H_4SiW_{12}O_{40}$ immobilized on polyaniline. Hydrophobicity and a greater affinity of HPA onium solids towards the non-polar isobutene, as compared to pure HPA, enhances *t*-BuOH formation and, consequently, lowers the selectivity to ETBE (around 80%), compared to the 100% reported for pure HPA. However, no deactivation is observed with oniumsilica-supported HPA.

Several catalysts related to oniumsilica-immobilized HPA have been reported earlier. These catalysts were based on aminopropylated silica and Keggin ions for acid catalysis [38–41], or oniumsilica and polyoxometalates for liquid-phase oxidation catalysts [42]. Interestingly, a similar approach was used earlier for immobilization of the Lewis acids, $SnCl_4^-$ [43] and $AlCl_4^-$ [44], on tetraethylammonium-, pyridinium- and *N*-methylimidazolium-silicas.

3.4.2. Synthesis of ethyl acetate

In our work, esterification of acetic acid at 60 °C was catalyzed by **MeIm-HPA** and **BuIm-HPA**. Conversion of acetic acid was measured after 20 h. The activity is expressed as the number of moles of ester formed per mole of Keggin anion per hour. All catalysts tested are active in this reaction (Table 5). The activities per anion of the catalysts derived from $H_3PMo_{12}O_{40}$ [**MeIm-PMo** 7.2 h^{-1} and **BuIm-PMo** 10.0 h^{-1}] appear to be the lowest. The activities of the $H_4SiMo_{12}O_{40}$- and $H_3PW_{12}O_{40}$-based catalysts are twice as high. As in ETBE synthesis, where the tetraprotic acid $H_4SiW_{12}O_{40}$ exhibits the highest activity, the tetraprotic acid $H_4SiMo_{12}O_{40}$, when

Table 5
Catalytic activity of imidazolium-HPA-silicas (0.2 g) in esterification of acetic acid (8 mmol) at 60 °C, 20 h. TON—turnover number, total mol product per anion. Values in parentheses correspond to recycling tests.

Sample	Conversion (%)	Selectivity (%)	Mol product per KU per h	TON (ac^{-1})
MeIm-PMo	15.5	100	7.2	144
MeIm-PW	36 (29)	100	16.7	335
MeIm-SiMo	45	100	16.4	327
BuIm-PMo	29	100	10.0	200
BuIm-PW	73 (66)	100	23.9	479
BuIm-SiMo	68	100	24.7	494

immobilized on oniumsilicas, is highly active. This can result from the greater number of protons per Keggin unit of the tetraprotic acid $[(\mathbf{MI})_{2.4-2.9}\mathbf{H}_{1.6-1.1}\mathbf{SiMo_{12}O_{40}}]$ [1]. Indeed, ^{31}P NMR chemical shifts of TEPO adsorbed on **MeIm-SiMo**, **BuIm-SiMo** catalysts (as well as for **Py-1-SiW** and **Py-2-SiW** catalysts) confirm that its acidity strength is higher than that of the other acids. Furthermore, 3- and 4-charged heteropolyanions are capable of providing an additional stabilizing effect on the intermediate organic cations, and this effect is more pronounced for the "softer" 4-charged anion.

The activities of HPAs immobilized on γ-propyl-*N*-butyl imidazoilum silica are 1.5 times greater than when they are on γ-propyl-*N*-methyl imidazoilum silica. Perhaps this is because the bulkier and more hydrophobic cation contributes positively to the diffusion of reactants towards the active site and increases the activity per Keggin unit.

HPA concentrations in the spent **BuIm-PMo** and **MeIm-PMo** samples indicate partial loss of the acid during the reaction (after two consecutive tests): 34.7 and 6.4%, respectively, of the amount initially grafted (Tables 1 and 2). Recycling tests, performed with the two most active catalysts, demonstrate that the activity decreased by 9–20%, whereas the concentration of grafted PW decreased by 5–6% (Tables 1 and 2).

The obtained esterification results are comparable to those reported for related immobilized HPA catalysts. The activities of the catalysts studied here vary from 7 to 25 h^{-1}. This is higher than reported for carbon-immobilized $H_4SiW_{12}O_{40}$ (activity per anion, 3.6 h^{-1}) and $H_3PW_{12}O_{40}$ (activity per anion, 6 h^{-1}) in the esterification of propanoic acid with butanol and 2-ethylhexanol in toluene at 60 °C, respectively [17]. The results are, however poorer than those obtained with MCM-41-immobilized $H_4SiW_{12}O_{40}$ and $H_3PW_{12}O_{40}$ (activity per anion varies from 200 to 250 h^{-1} in the liquid-phase esterification of benzoic acid with propan-1-ol in toluene) and parallel to the activity of MCM-41-immobilized HPAs (TOF 40 h^{-1}) in the gas-phase esterification of acetic acid with butan-1-ol [36]. However, in this case the catalysts suffered from serious HPA leaching.

4. Conclusion

Keggin heteropolyacids ($H_3PMo_{12}O_{40}$, $H_3PW_{12}O_{40}$, $H_4SiMo_{12}O_{40}$ and $H_4SiW_{12}O_{40}$) were immobilized on functionalized silica as their onium (propylpyridinium and alkylimidazolium) salts. Interaction between HPA and the surface-grafted onium cations affords acid salts. Tetraprotic acids, $H_4SiW_{12}O_{40}$ and $H_4SiMo_{12}O_{40}$, give better surface exchange yields and result in solids with greater acid site number per anion and strength. The major part of immobilized PW, SiW, PMo and SiMo anions in the as-prepared and spent catalysts samples preserve Keggin structure. Immobilization of $H_3PMo_{12}O_{40}$ is accompanied by partial decomoposition (up to ca. 0–5%).

In the two model reactions tested, the gas-phase synthesis of ETBE and the liquid-phase esterification of AcOH with EtOH, the materials display good catalytic performance: high activity (activity per anion, up to 150 and 25 h^{-1}, respectively), good selectivity (around 80% and 100%, respectively) and relatively good structural stability. Indeed the resistance to HPA leaching is significantly better than for the silica-supported HPA materials, the best hydrolytic stability being found for $H_4SiW_{12}O_{40}$.

The method used to graft the onium cation onto the silica and the nature of the cation slightly influences catalyst performance. Catalysts having a greater coverage (as shown by comparing two pyridinium salts) and hydrophobic cations (as shown by comparing two imidazolium salts) are preferable. Amongst the heteropolyacids studied, $H_4SiW_{12}O_{40}$ is the most active and promising for catalyst design.

References

[1] T.V. Kovalchuk, Ph.D. thesis, Pierre et Marie Curie University, Paris, France, 2003.
[2] F. Cunill, M. Vila, J.F. Izquierdo, M. Iborra, J. Tejero, Ind. Eng. Chem. Res. 32 (1993) 564.
[3] K.W. Otto, Oil Gas, January 11, 1993.
[4] T. Nishina, Shokubai Catal. 186 (1994) 36.
[5] T. Deguchi, Petrotech 15 (1992) 874.
[6] C.P. Nicolaides, C.J. Stotijn, E.R.A. Van der Veen, M.S. Visser, Appl. Catal. A 103 (1993) 223.
[7] J.S. Kim, J.M. Kim, G. Seo, N.C. Park, H. Niiyama, Appl. Catal. 37 (1988) 45.
[8] G.M. Maksimov, I.V. Kozhevnikov, React. Kinet. Catal. Lett. 39 (1989) 317.
[9] S. Shikata, T. Okuhara, M. Misono, Sekiyu Gakkaishi 37 (1994) 632.
[10] G. Baronetti, L. Briand, U. Sedran, H. Thomas, Appl. Catal. A 172 (1998) 265.
[11] Y. Ono, T. Baba, in: Proc. 8th Int. Congr. Catal., Berlin, Germany, vol. 5, Verlag Chemia-Dechema, Weinheim, 1984, p. 405.
[12] A. Agrachi, T. Matsuda, Y. Ogino, Sekiyu Gakkaishi 22 (1979) 331.
[13] A. Bielanski, R. Dziembaj, A. Malechka-Lubanska, J. Pozniczek, M. Hasik, M. Drozdek, J. Catal. 185 (1999) 363.
[14] M.H. Matouq, S. Goto, Int. J. Chem. Kinet. 25 (1993) 825.
[15] O. Françoise, F.C. Thyrion, Chem. Eng. Process. 30 (1991) 141.
[16] N. Mizuno, M. Misono, Chem. Rev. 98 (1998) 199.
[17] P. Dupont, F. Lefebvre, J. Mol. Catal. 114 (1996) 299.
[18] M.A. Schwegler, H. Van Bekkum, N.A. Munck, Appl. Catal. 74 (1991) 191.
[19] M.J. Verhoef, Microporous Mesoporous Mater. 27 (1999) 365.
[20] W. Chu, X. Yang, Y. Schan, X. Ye, Y. Wu, Catal. Lett. 42 (1996) 201.
[21] J.P. Osegovic, R.S. Drago, J. Catal. 182 (1999) 1.
[22] H. Niiyama, Y. Saito, et al., in: Proc. 7th Int. Congress Catal., Kodansha, Japan, Elsevier, Amsterdam, 1980, p. 1417.
[23] T. Baba, H. Watanabe, Y. Ono, J. Phys. Chem. 87 (1983) 2406.
[24] S. Shikata, T. Okuhara, M. Misono, J. Mol. Catal. A Chem. 100 (1995) 49.
[25] T. Okuhara, T. Nakato, Catal. Surv. Jpn. 2 (1998) 41.
[26] M. Kimura, T. Nakato, T. Okuhara, Appl. Catal. A 165 (1997) 227.
[27] B. Bardin, R. Davis, Top. Catal. 6 (1998) 77.
[28] T. Okuhara, T. Yamada, K. Seki, K. Johkan, T. Nakato, Microporous Mesoporous Mater. 21 (1998) 637.
[29] N. Essayem, G. Coudurier, M. Fournier, J. Vedrine, Catal. Lett. 34 (1995) 223.
[30] M. Misono, in: B. Imelik (Ed.), Catalysis by Acids and Bases, Elsevier, Amsterdam, 1985, p. 147.
[31] A. Corma, Chem. Rev. 95 (1995) 592.
[32] S. Damyanova, J.L.G. Fierro, I. Sobrados, J. Sanz, Langmuir 15 (1999) 469.
[33] W. Yang, J. Billy, Y. Ben Taarit, J.C. Vedrine, N. Essayem, Catal. Today 73 (2002) 153.
[34] F. Babou, G. Coudurier, J.C. Vedrine, J. Catal. 152 (1995) 341.
[35] N. Essayem, A. Holmquist, G. Sapaly, J.C. Vedrine, Y. Ben-Taarit, Stud. Surf. Sci. Catal. 135 (2001) 1991.
[36] M.J. Verhoef, P.J. Kooyman, J.A. Peters, H. Van Bekkum, Microporous Mesoporous Mater. 27 (1999) 365.
[37] A. Bielanski, A. Lubanska, J.J. Pozniczek, A. Micek-Ilnicka, Appl. Catal. A 238 (2003) 239.
[38] V.N. Zaitsev, T.V. Kovalchuk, J. Fraissard, in: Proc. of the Congress "Functionalized Materials", Kiev, Ukraine, 2002, p. 118;
T.V. Kovalchuk, V.N. Zaitsev, P. Batamack, H. Sfihi, J. Fraissard, in: Congress "Silica 2001", Mulhouse, France, September 2001, CD-ROM Proceedings;
T.V. Kovalchuk, V.N. Zaitsev, J. Fraissard, in: Proc. 4th Int. Symp. Supported Reagents and Catalysts in Chemistry, St. Andrews, UK, July 2000, p. 40.

[39] M. Kamada, H. Kominami, Y. Kera, Colloid Interface Sci. 182 (1996) 297.
[40] M. Kamada, H. Nishijima, Y. Kera, Bull. Chem. Soc. Jpn. 66 (1993) 3565.
[41] Y. Kera, M. Kamada, Y. Hanada, H. Kominami, Compos. Interfaces 8 (2001) 109.
[42] T. Kovalchuk, H. Sfihi, V. Zaitsev, J. Fraissard, J. Catal. 249 (2007) 1.
[43] T.M. Jyothi, M.L. Kaliya, M. Herskowitz, M.V. Landau, Chem. Commun. 11 (2001) 992.
[44] M.H. Valkenberg, C. de Caestro, W.F. Hoelderich, in: Proc. 4th Int. Symp. Supported Reagents and Catalysis in Chemistry, St. Andrews, UK, July 2000, pp. 242–247.